Three Stage Design Analysis and Multi-criteria Optimization of a Parallel Ankle Rehabilitation Robot Using Genetic Algorithm

Prashant K. Jamwal, Shahid Hussain, and Sheng Q. Xie, Senior Member IEEE

Abstract— This paper describes the design analysis and optimization of a novel 3-degrees of freedom (dof) wearable parallel robot developed for ankle rehabilitation treatments. To address the challenges arising from the use of parallel mechanism, flexible actuators and the constraints imposed by the ankle rehabilitation treatment, a complete robot design analysis is performed. Three design stages of the robot, namely, kinematic design, actuation design and structural design are identified and investigated and in the process six important performance objectives are identified which are vital to achieve design goals. Initially the optimization is performed by considering only a single objective. Further analysis revealed that some of these objectives are conflicting and hence these are required to be simultaneously optimized. To investigate a further improvement in the optimal values of design objectives, a preference based approach and evolutionary algorithm based non-dominated sorting algorithm (NSGA II) are adapted to the present design optimization problem. Results from NSGA II are compared with the results obtained from the single objective optimization and preference based optimization approaches. It is found that NSGA II is able to provide better design solutions and is adequate to optimize all the objective functions concurrently. Finally, a fuzzy based ranking method has been devised and implemented in order to select the final design solution from the set of non-dominated solutions obtained through NSGAII. The proposed design analysis of parallel robots together with the multiobjective optimization and subsequent fuzzy based ranking can be generalized with modest efforts for the development of all the classes of parallel robots.

NTP: Design of parallel robotic mechanisms present many challenges. This papers attempts to formulate and solve these problems in the pretext of

P. K. Jamwal is with the Department of Mechanical Engineering, Rajasthan Technical University, Kota, India (e-mail: pjam025@aucklanduni.ac.nz).

S. Hussain is with the Department of Robotics and Mechatronics, Nazarbayev University, Astana, Kazakhstan (e-mail: shahid.hussain@nu.edu.kz).

S. Q. Xie is with the Department of Mechanical Engineering, The University of Auckland, Auckland, New Zealand (e-mail: s.xie@aucklanduni.ac.nz).

a parallel mechanism designed for ankle joint physical therapy. The problems include the parallel mechanism itself and intrinsically compliant or flexible actuators used to power the parallel robot. In order to address these issues, a complete design analysis of the parallel ankle rehabilitation robot was carried out. The design analysis was divided into three stages namely, kinematic design, actuation design and structural design. A NSGA II algorithm was used to optimize the six performance objectives. The method proposed in this work can be used for the development of all categories of parallel robots with minor adaptations.

Index Terms—Wearable Ankle rehabilitation robot, parallel robots, robot design optimization, non-dominated genetic algorithm

I. INTRODUCTION

SEVERAL robotic platforms based on parallel mechanisms have been developed to impart repetitive physical therapy to the patients suffering from ankle joint disorders. In one of the earliest works in this direction, Girone et al. proposed the Rutgers Ankle that used a Stewart platform, capable of providing six dof to the ankle joint [1]. Although Rutgers Ankle has been developed and is being used for scientific experiments, its redundant actuation is a drawback. In order to reduce the redundancy of the above Stewart platform, Dai et al. [2, 3] proposed a parallel robot for sprained ankle treatments using a three and four dof parallel mechanisms. Another instance of parallel robot used for ankle joint rehabilitation is found in [4] where a single platform-based reconfigurable robot mechanism has been proposed. A 3-RSS/S parallel mechanism is proposed by [5] and the kinematic design of its prototype is validated using simulations. Lately, Syrseloudis and Emiris [6] have proposed a tripod based parallel robot actuated by electric motor, after evaluating several serial and parallel robot solutions for the ankle rehabilitation robot.

More or less all these platform type robots require patient's foot to be placed on top of a table which is actuated from the bottom. These robots have a fixed base and are heavy thus are not ergonomic designs. Apart from the portability issue, non-compliant actuations and higher costs, there are certain other pragmatic issues with such configuration. Firstly, since the robot end-effector containing the patient's foot (fixed on top of the table) is moved by placing actuators below the table, the position of the ankle joint and the shinbone keeps changing with respect to the ground (Fig. 1). This instability in the position of the ankle joint leads to control errors which are difficult to comprehend. Secondly, these designs do not remain kinematically compatible with the ankle joint during motions owing to their heavy weights and placement of actuators [7]. To overcome above mentioned limitations of ankle robotic platforms a novel parallel robot has been developed by the authors and readers are referred to [8] for further details of the mechanism. The robot design is biologically inspired and is therefore kinematically compatible with the ankle joint motions. Inherently compliant pneumatic muscle actuators (PMA) have been deployed along with cables in this robot to achieve compliant actuation and safe operation. The ankle robot is light weight, portable and compact and hence is wearable.

This wearable ankle robot set forth design challenges with regards to its wearability requirement, use of parallel mechanism, cable based actuation and clinical requirements for ankle joint rehabilitation treatments. Wearability can be further explained in terms of requirements such as light weight, compact design, comfortable in use, safety and portability. While using parallel mechanisms for the robot, issues such as, smaller workspace and singularity were needed to be addressed. Cable based actuation imposed a constraint that the robot motion be achieved through positive actuator forces and the stiffness of the robot be analyzed

in context to its rigidity. Finally, the robot's application in the ankle joint rehabilitation stipulated higher actuator force requirement and set forth design constraints arising from its use by subjects of varying physical abilities. In the light of these challenges, it was desired that the robot design be analyzed from above mentioned aspects and some performance objectives be identified in order to find an appropriate trade-off between objectives and achieve an optimum design.

Design optimization of parallel robots is normally performed using trial and error approach. Optimized design solutions are obtained by carrying out rigorous experiments or simulation runs and intuitive judgments on the results thereafter. However, using such approach, the required number of simulation runs increases exponentially with an increase in number of design objectives. Moreover tuning of all the design criteria simultaneously is difficult and time consuming. Previous research also includes optimization of one or more of the design objectives using numerical methods [9]. Several performance objectives or design criterion such as manipulability, isotropy, dexterity index, conditioning index, global conditioning index and global isotropy index have been described and optimized by different researchers [9] in order to obtain an optimal robot design.

(a)   (b)
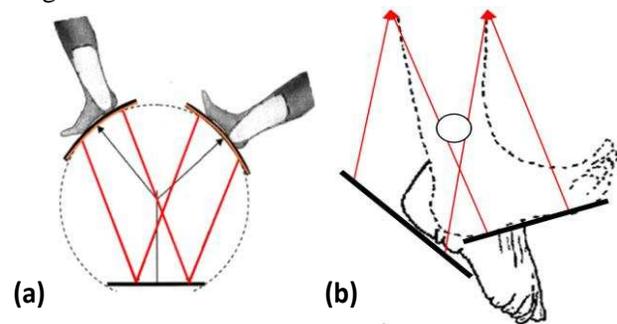
Figure 1: (a) Changing foot and ankle positions in platform type parallel robots (b) Proposed anatomically correct arrangement of actuators to maintain ankle joint stationary. Actuators are shown by red lines.
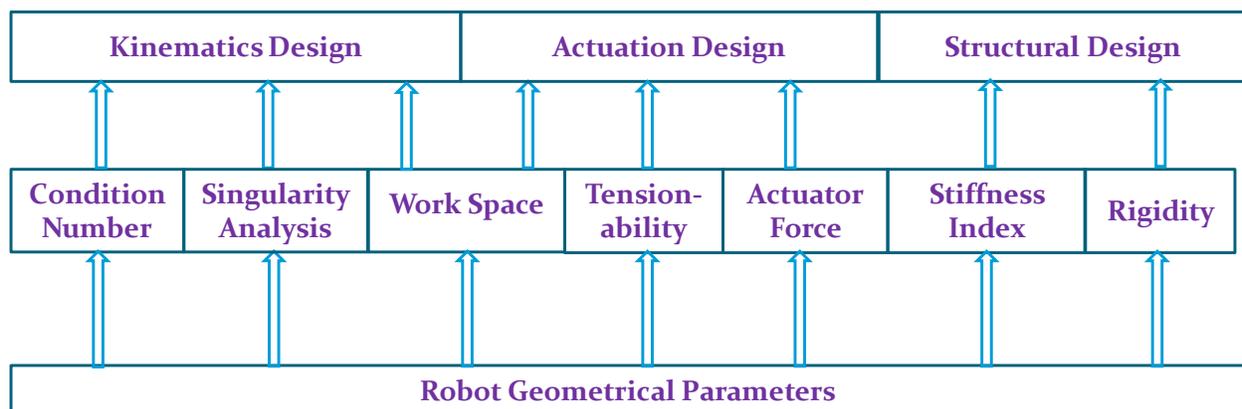
Figure 2: Three design stages (Kinematic, actuation and structural) of the ankle robot and related performance objectives.

In one of the pioneering works, architectural optimization of a 3-dof parallel robot has been performed by [10] to maximize the global conditioning index. GA has been used with constraints defined as penalty functions by [11] to minimize the minimum condition numbers in the entire workspace. To validate and verify the algorithm, results obtained from GA have further been compared with the Quasi-Newton method. Global conditioning index has been optimized as a result of altering the length of links by [9].

The authors have used a nested implementation of two GA to obtain a mini-max genetic solution. A performance index called space utilization has been proposed by Stock and Miller to evaluate the optimal kinematic design of a linear Delta robot [12]. They have used an exhaustive search minimization method to optimize mobility, workspace and manipulability. A branch and prune type algorithm has been used by Merlet [13] to optimize workspace and stiffness of a modular parallel robot and improve its performance. A kinematic design method has been implemented by [14] and various performance objectives such as global conditioning workspace, global conditioning index and global stiffness index have been used to obtain the optimal design. Genetic algorithm (GA) has been used by [15] to optimize the workspace of a 2- dof parallel robot using a single objective function. In order to optimize actuator forces in a cable based parallel manipulator, Hassan & Khajepour [16] proposed to use Dykstra's projection method. Though the force distribution among links has successfully been optimized to provide minimum norm solution, the robot design has not been altered to minimize the actuator forces.

Multi-criteria optimization has also been carried out by researchers in past and in this context use of interval analysis to obtain optimal design of a parallel robot is vital [17]. All possible solutions satisfying the design constraints have been obtained; the best design compromise is determined later by sampling the solution regions. A weighted average approach has been given by Lemay & Notash [18] wherein they have proposed a combination of GA and simulated annealing algorithms to optimize workspace, dexterity and mass & size of the manipulator simultaneously. Normal Boundary Intersection (NBI) method [19] is applied to efficiently obtain the Pareto hyper surface for a five linkage parallel robot. NBI solves the multi-objective optimization problem by constructing several aggregate objective functions (AOF). The solution of each AOF yields a Pareto point, whether locally or globally. However, according to Erfani and Utyuzhnikov [20], there are approaches such as Directed Search Domain (DSD) method and evolutionary algorithms which are more efficient than NBI.

Subsequently, some early attempts have been made to perform design optimization of parallel robots using evolutionary algorithms [21-23]. However these research efforts have been limited to a few specific performance criteria to achieve specific design goals. Recently some research work has been done in the field of parallel robot design optimization [24-26], however our work differs from the work presented in a manner that we work with robot which has cable based redundant actuation. Contrary to the earlier endeavors, present research work aims to conduct a systematic design analysis of the parallel ankle robot. Efforts have been made, in this research, to lay down an organized procedure for the design analysis of a specific parallel robot which can be easily generalized and adopted for all kinds of parallel robots. To the best knowledge of authors, this is a first ever attempt, in the field of parallel mechanisms, wherein a staged design analysis has been developed and performed into three levels of hierarchy namely, kinematic, actuation and structural design. Several performance objectives have also been developed in the process and the robot design has been defined in terms of its geometrical variables. Multiobjective optimization (MOP) based on evolutionary algorithms has been implemented using non-dominated sorting genetic algorithm (NSGA-II) to obtain optimal robot. Results from the NSGA II have been compared with results obtained from two other optimization approaches namely; single objective optimization and priority based MOP to demonstrate the significance of multiobjective evolutionary design optimization.

II. DESIGN ANALYSIS

Following an initial analysis of the robot mechanism and referring the literature [27-29], seven important objectives were identified encompassing three main aspect of the robot design namely; kinematic design, actuation design and structural design (Fig. 2). Singularity analysis and condition number of the robot's Jacobian matrix along with the isotropic workspace of the robot were considered to be investigated for its kinematic design aspect. It is important to note here that the robot workspace determination is governed by two aspects of the robot design namely, kinematic and actuation design. Therefore, while investigating the actuation design aspect, apart from the other requirements, workspace of the robot was also carefully studied. Finally the structural design aspect was examined in context to the stiffness and rigidity of the ankle robot. The relation between these objectives and their respective design aspects have been shown in Fig. 2. The objectives are not mutually independent rather they are inter-reliant while some of them even

conflicting. The interdependence of objectives and their dependence on condition number is shown in Fig. 3.
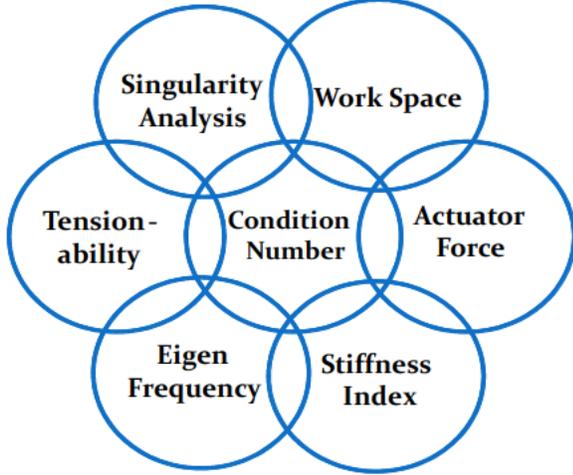
Figure 3: Interdependency of the performance objectives

It has been established and shall be verified later in this work that the geometrical parameters of a parallel robot affect the robot condition number which eventually affects above mentioned objectives [13]. This Section defines robot design parameters and formulates objectives mathematically.

A. Robot geometrical parameters

The study of the robot design in the present work has been fundamentally the analysis of its geometry, which is mainly defined by the configuration of actuator connection points on the two platforms and the separation between the platforms of the parallel ankle robot. Effective shapes and sizes of the platforms are decided by these connection points and the height of robot is governed by the distance between the platforms. The geometrical design parameters of the robot have been considered as the optimization variables and are illustrated in Fig 4. Different robot designs can be obtained by varying the polar coordinates of the connection points on both the platforms. The objective is to find the best design from the infinite number of possible constellations of actuator connection points. The feasible area on the platforms is the region which is available after applying the requisite constraints given below (1-3).

It is apparent that the solution space, after applying the constraints, is a continuous region which can be investigated by changing the polar coordinates. Parameters $q1, q3, q5$ and $q7$ are the angular positions of the actuator connection points (on the other hand $q2, q4, q6, q8$ are the radial distances of the connection points from centres of the two platforms) on both, the fixed as well as moving platforms. In order to maintain the symmetry the connection points are also kept symmetric and as such connection points on the two halves of the platforms are mirror images. The limiting values of

parameters $q_1, \ldots, q_8$ (1&2) have been carefully decided by leaving sufficient space for patients to conveniently place their foot on the robot end-effector. A total of eight design parameters have been selected which are the polar coordinates of actuator connection points (A&A', B&B' etc.) with respect to the centers of both the platforms (Fig. 4). Distance between the platforms has not been changed and is kept as 120 mm, which is the expected distance of ankle joint from the foot base. Owing to the limitations arising from the use of ankle robot by variety of subjects, following geometrical constraints have been considered. The limits on geometrical constraints are in millimeters and radians (1-3).

$$\frac{\pi}{12} \leq q_1, q_3 \leq \frac{\pi}{3} \quad and \quad \frac{\pi}{12} \leq q_5, q_7 \leq \frac{4\pi}{9} \tag{1}$$

$$80 \leq q_2, q_6, q_8 \leq 120 \quad and \quad 120 \leq q_4 \leq 160 \tag{2}$$

Additionally, actuator stroke length constraint (3) for the PMA has also been considered.

$$max(l_p^o) - min(l_p^o) \leq 110 \quad for \quad p = 1, \ldots 4. \tag{3}$$

Here, l_p^o is the length of pth cable of the robot and $q_i's$ are the geometrical parameters shown in Fig 4.

B. Kinematic Design

The ankle robot is made up of two parallel platforms which are connected together with four links (Fig. 4).
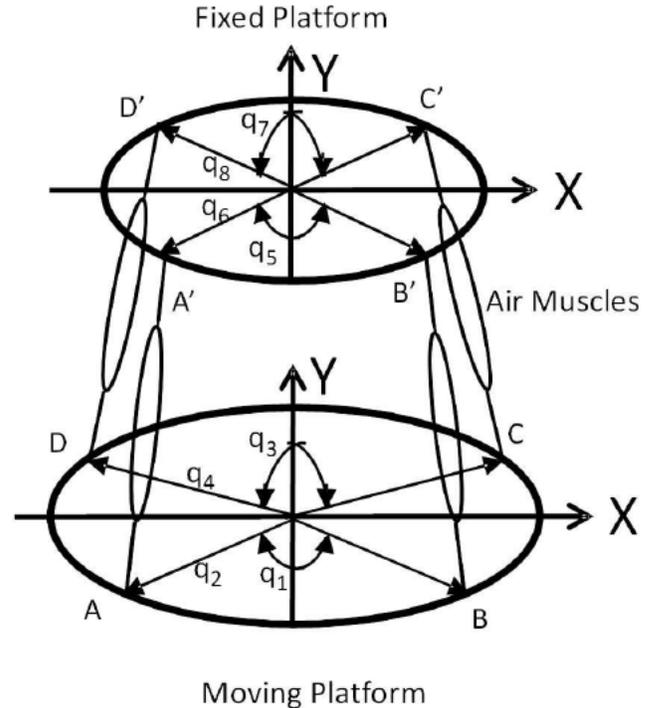
Figure 4: Geometrical parameters of the moving platform and the FP of the ankle robot

Thus the kinematic structure of the robot has four closed kinematic pairs and the robot motions are achieved through simultaneous motion of these kinematic pairs. While designing the wearable robot, its geometrical parameters, which define positions of these

kinematic pairs, have been carefully selected in order to avoid the robot configuration becoming singular. The condition number of the robot's Jacobian matrix, which is also a measure of singularity, provides a relation between changes in the joint space and task space kinematic variables.

Condition number is an important robot design parameter and solely depends on robot's physical construction. Condition number and singularity aspect of the wearable robot are further discussed in view of their overall significance and dependence on robot's geometrical construction.

1) Condition Number

The mapping of joint velocities to its Cartesian velocities for a robot is done using robot's Jacobian matrix (J). The condition number of this Jacobian matrix has important physical significance [30-32].   A robot design with near unity condition number is desirable [9] since it minimizes the error in the end-effector torque due to input error in joint wrench. The condition number can also be used to evaluate the workspace singularities. It reveals how far the robot is from its present configuration to the nearest singular configuration. Eventually, the condition number is a vital design parameter and the robot configuration should be optimally designed to acquire a condition number close to unity. To evaluate the robot design, condition number is generally obtained at different workspace points on the specified robot trajectory with assumed resolution. Though condition number (k) at different end-effector orientation is useful information, to get a comprehensive view of its distribution in the entire workspace volume, a Global Condition Number (GCN) given by (4) is normally used [33-35].

$$GCN = \frac{\sum_{i=1}^{n}(k)}{n} \tag{4}$$

Here n is the total number of discrete feasible points constituting the workspace and the numerator is the sum of condition numbers obtained at these points in the feasible workspace volume grid. Similar to the condition number, GCN is bounded by the range as given below.

$$1 \leq GCN \leq \infty \tag{5}$$

2) Singularity Analysis

During the course of its motion, the ankle robot which works on parallel mechanism, sometimes enters into a configuration wherein, instantaneously, it gains or losses extra degrees of freedom [28]. This configuration of the robot is referred to a singular configuration and as a result robot loses its stiffness and become uncontrollable. This phenomenon can be best explained using robot Jacobian matrix as below.

Link velocities $\dot{q}$ of the robot actuators can be directly mapped into the twist vector t of the robot end platform.

$$X\dot{q} = Yt \tag{6}$$

The Jacobian matrix, J(q) of the robot which symbolizes this mapping, can be further defined as below.

$$J = X^{-1}Y \tag{7}$$
$$\dot{q} = J(q)t \tag{8}$$

A close inspection of (7) reveals that X^{-1} is a square matrix and always has a solution, on the other hand matrix Y is a 4×3 matrix and can be rank deficient. Therefore, rank of Jacobian matrix J is decided by the rank of matrix Y. In other words, matrix J will be singular when matrix Y is also singular. Subsequently, matrix Y was analyzed to deduce inferences regarding the configurations and geometries of the robot where it will enter into singularity.

In this work a different method has been used whereby the rank behaviour of matrix Y is analyzed with regards to its invertibility and the outcomes are supported by simulation results.

Matrix Y can be deduced as (9) to further explain its rank analysis.

$$Y = \begin{bmatrix} (a_i^o \times L_i^o)^T \\ \ldots. \end{bmatrix} \tag{9}$$

Here a_i^o is the position vector of the actuator connection at fixed platform of the ankle robot. The link vector L_i^o can be expressed in terms of position vector of the ankle joint and link connection points on the two platforms as (10).

$$L_i^o = (P_e^o + R_e^o a_i^e - b_i^o) \tag{10}$$

It can be easily shown that when $R_e^o = I$ and $a_i = \mu b_i$ i.e. when the two platforms have same orientation and proportional dimensions, all four lengths of the robot would be equal. It is important to note here that the full rank of matrix Y (which is a 4×3 matrix) is three when its columns are independent. However during instances when all the lengths are equal, only two columns of Y remains independent and its rank become two. Inverse of matrix Y in such case does not exist as it has become rank deficient. As a result, Jacobian matrix (7) also becomes rank deficient. Interestingly, the minimum singular value in this case becomes zero and the condition number of the Jacobian matrix, which is the ratio of largest singular value to the smallest singular value, in such instances becomes infinite. This inference can be further validated from the simulation results shown in Fig. 5, where condition number distribution is shown at various robot orientations. The geometrical parameters of the robot are chosen so that the condition $a_i = \mu b_i$ holds true. End-effector was moved about the three axes in the space, sequentially at an interval of 3 degrees starting from zero. Thus a total of 33

configurations were studied. Apparently, condition number values become infinite at the beginning of each cycle of robot motions (orientations 1st, 12th, 23rd) when the two platforms are aligned or $R_e^o = I$. Condition number values at other orientations are also very high which are not acceptable. Therefore, in the light of above findings, it is recommended that following arrangements of robot geometry should be avoided while designing the parallel robot.

Case I: The two platforms are of same size and have same orientations.

Case II: The two platforms are of slightly different size but have same orientations.

Case III: The two platforms are of different size and have zero separation or are coincident.

Case IV: The two platforms are of different size but are in the same plane.
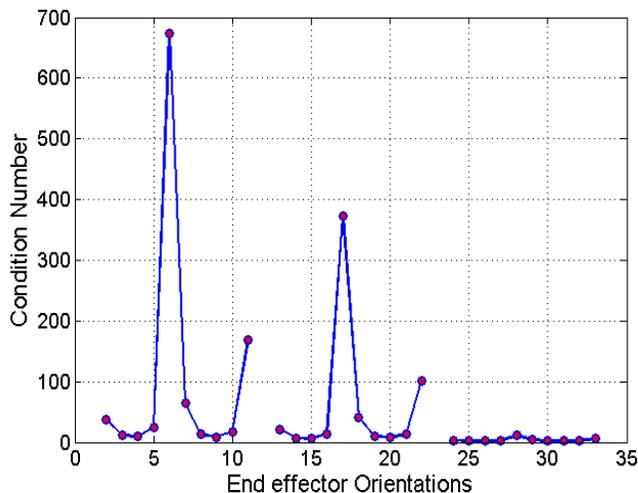
Figure 5: Condition number distribution versus index of end-effector orientations in the workspace.

C. Actuation Design

The ankle robot is actuated using PMA in series with cables. These PMA are flexible actuators which can provide pull/tension forces but fail to supply compressive forces. Thus use of PMA and cables for actuation of the robot requires that during its course, the robot end-effector orientation be achieved with positive forces or tensions in the links, failing which the robot loses controllability. This requirement has been named as tensionability and is further explained in the following subsection. Appropriate placement of the actuators is important in achieving tensionability.

Comprehensive workspace of the wearable robot is a subset of the constituent workspaces from individual kinematic pair and hence is governed by robot's geometrical design which includes parameters such as lengths and placements of its links and actuators. While working out actuator forces, it is explicable that, to realize required moments at the end-effector, the

actuator forces largely depend on the placement of actuator connection points on the two platforms which defines robot design. Apparently when the actuators are connected close to the robot's centre of rotation, the forces to realize certain moment at the end-effector are large compared to when the actuators are placed farther. The force closure, workspace and the actuator forces are further analyzed under the actuation design aspect of the robot and discussed in the following subsections.

1) Force Closure and Tensionability

The requisite moments by which the robot end-effector is moved are realized by providing suitable forces in four actuators. Apparently when the force closure is solved for certain end-effector moment, a force vector, which has combination of positive and negative (or tensile and compressive) forces, is obtained for the actuator wrench (11). Here, a major constraint called tensionability is encountered as discussed below. A new method has been proposed in this research and a quadratic minimization algorithm has been used for the first time for force closure analysis of the parallel robots.

Cables used in conjunction with the PMA in the ankle robot have unidirectional properties i.e. they cannot provide compressive forces. Additionally, the flexible PMA can also provide only a positive or tension force. Thus the force closure obtained from (12) is not a feasible solution and some other means are to be explored to obtain a positive force vector. Further investigations revealed that, the redundant actuation in the present case provides an extra degree of freedom in the null space solution of the robot's Jacobian matrix (J). This makes it possible that the desired orientations and moments at the end-effector are achieved through with positive (or tension) forces in the cables. To carry out the force closure analysis, the joint space forces which can produce a particular task space moment vector can be obtained using (12). Further, since the task space has three degrees of freedom, realized by using four actuators, the resulting end-effector Jacobian matrix is a non-square matrix. It can be easily verified that there will be an infinite number of actuator force vectors (12) which can provide the requisite task space moment (11). The extra component of null space forces can be arbitrarily selected without influencing the actual task space torque. Therefore, the extra degree of freedom in the null space of robot's Jacobian matrix can be utilized to meet the tensionability constraint posed by cable actuation.

$$M_{ext} = J^T F \qquad (11)$$
$$F = \bar{J} M_{ext} \qquad (12)$$

Where $\bar{J} = J(J^T J)^{-1}$ is the pseudo inverse of J^T.

Next, at each point of the desired trajectory of the end-effector, forces in each cable are calculated

7

using equation (12). Since the pushing force is not possible from the actuators, a positive force vector for the cables can be obtained using a quadratic minimization algorithm [36]. Here M_{ext} is the target external moment applied to the platform and M_{res} is the moment resulting from the four actuator forces. Formulation of the optimization problem is explained below:

Without loss of generality, the moment provided by the resulting positive force vector can be written as (11). Comparing (11) with (13) then yield (14-16), where V_1 and U are matrices containing the input and output basis vectors corresponding to non zero singular values of J^T and V_0 is the null vector of J^T. Additionally, η is a vector specifying the components of ΔF along the column vectors of V_1 and ε is a scalar defining the component of ΔF along V_0.

$$M_{res} = J^T F_{res} \tag{13}$$
$$\Delta M_{ext} = M_{res} - M_{ext} \tag{14}$$
$$\Delta F = F_{res} - F = V_1 \eta + V_0 \varepsilon \tag{15}$$
$$J^T = U\Sigma \begin{bmatrix} V_1^T \\ V_0^T \end{bmatrix} \tag{16}$$

The relationship between (14) and (15) can be written as:
$$\Delta M_{ext} = J^T \Delta F \tag{17}$$
$$\Delta M_{ext} = U\Sigma \begin{bmatrix} V_1^T \\ V_0^T \end{bmatrix} [V_1\ V_0] \begin{bmatrix} \eta \\ \varepsilon \end{bmatrix} \tag{18}$$
$$\Delta M_{ext} = U[diag(\sigma_1, \sigma_2, \sigma_3)]\eta \tag{19}$$

From above analysis, following objective function can be deduced.

Minimize
$$\Delta M_{ext}^T \Delta M_{ext} = \eta^T[diag(\sigma_1^2, \sigma_2^2, \sigma_3^2)]\eta \tag{20}$$
Subjected to
$$\mu_l \leq F_{res} \leq \mu_u \tag{21}$$
$$\Rightarrow \mu_l \leq [(\bar{J})^T M_{ext} + \varepsilon V_0 + V_1\eta] \leq \mu_u \tag{22}$$

Thus during the optimization a force vector is obtained which lies in the constrained limits given by (21) and is able to provide the desired moments at the end-effector with minimum error. In the present work, lower bound (μ_l) of the actuator forces is consider to be zero and the upper bound (μ_u) is defined as force threshold, another objective function which is later minimized. Since the cables in the robot have been provided some pretension, the zero force in the cables added with the pretension actually provides a positive actuator force.

2) Robot Workspace Analysis

The workspace of the proposed cable driven robot is difficult to analyze for three major reasons. Firstly, the orientation workspace is achieved through coupled motion of its links or cables which is difficult to evaluate independently. Consequently, the workspace has been

defined simply as the space where the inverse and forward kinematic solutions exist [37]. Secondly, workspace for the cable driven robots [38], is defined as the conglomeration of points where sets of positive cable tensions is attainable, a condition which has been discussed in the preceding Section. Finally, the compact design requirement of the robot poses a constraint on the actuator lengths which in turn constraints the reachable workspace. Since the length of the wearable ankle robot is governed by the length of its actuators, a compact design requires that the actuator lengths should be kept short to keep the total length of the robot close to the size of patient's shinbone. The PMA, upon inflating can only expand to 30% of its normal length. Therefore, limiting the actuator length, the stroke length and the reachable workspace provided by the group of muscles also get constrained.

The feasible workspace has been computed by carrying out a singularity analysis for the robot's Jacobian matrix, checking the tensionability condition (discussed in the preceding Section) and observing the actuation constraint of the PMA at discrete workspace points. Mathematically, the feasible workspace index (I) is defined as below [39].
$$I = \frac{\varphi_f}{\varphi_T} \tag{23}$$
$$\varphi_T = (\theta_{max} - \theta_{min})(\phi_{max} - \phi_{min})(\psi_{max} - \psi_{min}) \tag{24}$$
Here φ_f is the feasible workspace which has been obtained after satisfying all above mentioned constraints and φ_T is the total orientation workspace with limiting values for Euler angles as θ_{-25}^{+25}, φ_{-40}^{+40} and ψ_{-30}^{+30}.

3) Robot Actuator Forces

Due to higher stiffness of ankle joint, higher actuator forces are required to realize the necessary moment at the task space or the end-effector. It is desired to keep the length of the robot and its actuators small for compactness of the robot structure. Apart from actuation limits, the capacity of air muscle to exert force also proportionally depends on its length i.e. longer PMA are required to realize higher actuator forces during ankle joint motions. Eventually to minimize the lengths of actuators the actuator force requirements should be reduced. Moreover, higher actuator forces may cause the cables to break or may also produce undesired elongation in the cable and the flexible PMA, adversely affecting the positional accuracy. Apparently, the actuator force is a function of robot's geometrical parameters. By selecting actuator connection points on the robot platforms farther from the axis of rotation, the actuator forces can be greatly reduced. Further, to minimize the actuators force vector it is necessary to present the values of force vector using a single number. Vector norms are generally used to represent vectors in a

single value. Three types of vector norms are generally used namely, 1-norm, 2-norm or ∞-norm. Within these three norms, 2-norm or Euclidean norm is more preferred [16] owing to its sensitivity towards changes in the larger force components. The 1-norm is equally sensitive to all the force components whereas ∞-norm is only sensitive to the changes in the largest force component. In the present study, 2-norm of the actuator forces has been considered which is given by the minimum norm solution of (11) and can be written as the left pseudo inverse (12). The limits of the actuator forces can be determined using singular value decomposition theorem and are given as following.

$$\frac{\|M_{ext}\|}{\sigma_1} \leq \|F\| \leq \frac{\|M_{ext}\|}{\sigma_3} \tag{25}$$

It is interesting to note that the magnitude of the upper limit of the actuator forces is governed by the minimum singular value σ_3 and the forces along the actuators can be reduced by maximizing this value. However, when the condition number is minimized, it is possible that the minimum singular value also gets increased and as a consequence the actuator forces may reduce. In the light of above discussion, Euclidean norm of the four actuator forces, averaged over the workspace points is considered as one of the objective functions to minimize.

4) Maximum Robot Actuator Forces

Even if the norm of forces is small, there's an apprehension that an individual actuator force may exceed the permissible limits posed by PMA. Thus it is desired that the maximum actuator force be also minimized along with the norm of actuator forces. The maximum actuator force in an individual link is given by (26).

$$F = \max(J(J^T J)^{-1} M_{ext}) \tag{26}$$

D. Structural Design

Stiffness was a major concern while designing the wearable robot, which is being actuated by flexible and compliant PMA. Though compliance is a desirable feature for the wearable robot, stiffness is essential for positional accuracy and stability. It is discussed in the following subsections that the robot's stiffness which is governed by actuator stiffnesses, is a function of its geometry defined by the placement of links and actuators. Owing to the inherent flexibility in the actuators and cables, it was also desired to evaluate the rigidity of the robot which can be defined using Eigen frequencies of the robot stiffness matrix. Eigen frequencies can be obtained using the Eigen analysis of the stiffness matrix. Robot's stiffness matrix and its rigidity aspects are further elaborated in the next subsections.

1) Robot Stiffness Conditioning Index

A robot actuated by cables is said to be stabilizable if the stiffness matrix of the robot is positive definite under any arbitrary external wrench [40]. Stabilizability is a condition which guarantees the stability of the robot in any circumstances under sufficient antagonistic forces. The stabilizability is necessary to be investigated since antagonistic forces from PMA are used in the proposed robot to actuate the end-effector. Cable driven robots exhibit two types of stiffness namely, active stiffness and structural stiffness [34]. The active stiffness is produced by the internal forces of the cables and the structural stiffness comes from the elasticity and the stiffness of the actuation system. Apparently, the effect of internal forces on the stiffness can be ignored since the elongation of the cables due to the internal forces is insignificant. Thus in the present application, the structural stiffness matrix consisting of two components i.e. cables, and PMA has been analyzed.

$$K = J^T S J \tag{27}$$

$$\text{Where} \quad S = \frac{dF}{dl} = \text{diag}(k_1, k_2, k_3, k_4) \tag{28}$$

The overall stiffness matrix of the robot, from its actuator stiffness's, is computed using the robot's Jacobian matrix (J) as shown above. Here K is the total stiffness of the robot, F is the cable force vector, l is the vector of link lengths consisting of cables and PMA and '$k_1 .. k_4$' are the stiffnesses of the individual links. Link stiffness here represents two stiffnesses in series, the elastic stiffness of the cable and the stiffness of the PMA. Since both are in series, the resultant stiffness is mostly dominated by the less stiff member which is PMA [41].

$$k = \frac{3P_g L}{2\pi n^2} \tag{29}$$

This relation can be further written in terms of actuator force as:

$$k = \frac{6F}{\left[3L - \frac{b^2}{L}\right]} \tag{30}$$

Here P_g is the internal gauge pressure, L is the length of the PMA, n is the number of turns for a single thread of the mesh of PMA, and b is the thread angle of the PMA mesh. This is an approximate model and has been used in the present research; however, value of b and therefore stiffness may vary depending upon the type of constituent elements of the PMA. The overall stiffness matrix K can be resolved in three matrices using singular value decomposition as shown in (31).

$$[K]_{3\times3} = [X^T]_{3\times3}[\Sigma]_{3\times3}[Y]_{3\times3} \tag{31}$$

$$K_{min} = \min(\text{diag}(\Sigma_1, \Sigma_2, \Sigma_3)) \tag{32}$$

Once again X and Y are orthogonal matrices and Σ is a diagonal matrix of three singular values as $(\Sigma_1, \Sigma_2, \Sigma_3)$. The minimum of these diagonal values is

the minimum value of actuator stiffness (32) which has been considered as an objective to be maximized in the present work.

Apart from being stiff, the robot structure should be sufficiently rigid to carry out various ankle rehabilitation exercises. The robot should be able to respond quickly to the real time input from the system dynamics and the interaction dynamics. Apparently, the rigidity is closely related to the open-loop natural frequencies of the robot. The natural frequencies (ω) are obtained by solving the generalized Eigen value problem considering the mass matrix of the robot and the stiffness matrix (33).

$$\omega = \mathrm{sqrt}(K(M^{-1})) \qquad (33)$$

III. Design Optimization

Aim of this research is to obtain a well conditioned robot having optimal values for all the other objectives as well. The proposed robot has four actuators and thus has eight connection points on the two platforms. Since all the connection points on the platforms are coplanar, position of each of them can be defined by two parameters, yielding 16 parameters in all. However since the robot is to be used for both right and left foot ankle treatments, hence it is desired that it should have left-right symmetry. In other words the actuator- attachment points on the right half of the platforms should be a mirror replica of the connection points on the left half of the platform. Consequently, the number of independent parameters reduces to half i.e. instead of 16 only 8 parameters $q_1, \ldots, q_8$ are to be considered. These eight design parameters have been illustrated in Fig. 4.

1) Single objective optimization

Investigation of the objectives, identified for ankle robot design evaluation, revealed that all the objectives are connected to the condition number of the robot's Jacobian matrix and thus condition number is an important objective to be optimized. Initially it is assumed that by minimizing the condition number, the Jacobian singularities can be reduced which will improve the feasible workspace. Actuator forces are likely to decrease and stiffness of the robot is expected to increase as a consequence of condition number optimization [39]. To begin with, the design optimization was performed by considering condition number as the sole objective or performance criterion. Genetic algorithm [39] was employed for the optimization and the results obtained from single objective optimization strategy were analyzed. Later from these results motivations were drawn for the implementation of a multi-objective optimization method.

Results from the GA-optimized design (Table 1) were analyzed and it was found that the measure of GCN and its distribution in the workspace is satisfactory. However higher actuator force norm, reduced feasible workspace and low stiffness were still a matter of concern [39]. It was found that the single objective optimization approach cannot provide a best compromised solution with regard to all the performance criteria. Moreover using a single objective approach, it is difficult to establish a trade-off between criteria which are of conflicting nature, such as the actuator force norm versus workspace and tensionability versus condition number. These facts supported the decision for using of a multi-objective optimization approach in the present case. Subsequently, various multi-objective optimization approaches were reviewed and to begin with, the preference based approach which is frequently used in design optimizations was implemented in the present design optimization problem as discussed in the next Section.

Table 1: Results from condition number optimization

Global Condition Number	Actuator Force Norm (N)	Workspace Utilization (%)	Stiffness (Nm^{-1})	Error in moments (Nm)
2.06	645.19	95.32	232	1.37E-14

2) Multiobjective optimization
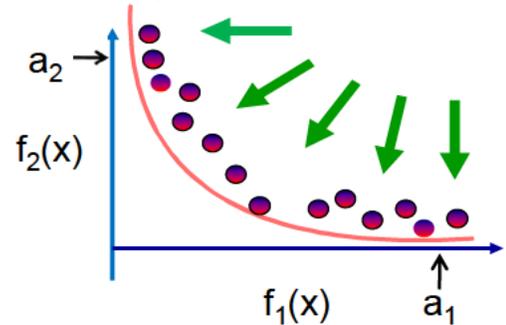
Figure 6: Pareto hypersurface solutions for optimization problem involving two objectives

Since the present optimization problems involve more than one objective, a single design solution may not be the best. A particular solution which provides best value of an objective may offer a compromised value for the other objective. The optimization goal in such design optimization problem is to obtain a cluster of solutions providing various grades and blends of the objective values. By grade and blends it is meant that different weights of objectives are grouped in different manners e.g. a2 $(0.1f_1, 0.9f_2)$ and a1 $(0.9f_1, 0.1f_2)$ as shown in Fig.6. Following this approach a Pareto hypersurface can be obtained as shown in Fig. 6, which contains solutions providing different grades and combinations of the objectives. There are basically two approaches to obtain

a Pareto hypersurface namely, preference based multi-objective optimization and Evolutionary Algorithm (EA) based multi-objective optimization.

While using the preference based approach a large number of optimization run would be required to construct the Pareto hypersurface, whereas the EA approach [42] is able to provide a Pareto hypersurface in a single run of the optimization. Initially the preference based optimization is performed; objectives are grouped to form a single-objective and then optimized. This is achieved by assigning a numerical preference index to each objective (performance index) and then combining the values of these preferences into a single value by either adding or multiplying all the weighted criteria [43]. In the present case, a candidate solution (V) is typically given by the formula as shown in (34).

$$V = w_1 \times f_1 + w_2 \times f_2 + \cdots + w_n \times f_n \qquad (34)$$

Here w_n is the preference assigned to function f_n where n is the total number of objective functions. This approach has several inherent advantages, such as; the significance of one objective over the rest can be regulated using appropriate preferences. Owing to its simplicity in implementation, this approach is very popular among designers. However it has certain shortcomings and worse of them is the ad-hoc selection

objectives were preferred. Perceptibly best individual objective values, at the cost of other objectives, are obtained when they are given more preference.

As explained above, the preference based approach is simple to implement and provides a mean to regulate preferences of objectives as per user's requirements. However in some instances where it is difficult to decide the priorities among objectives, this approach cannot be recommended. In the present case of design optimization the objectives are interdependent and conflicting, hence it is not possible to decide the vector of weights or the preferences for individual objectives. The arbitrary chosen weight vector may not be a good choice. Therefore, an EA based multi-objective optimization approach which evolves better solutions (in terms of their objective function values) equally and simultaneously is explored in the next step.

IV. NON-DOMINATED SORTING GENETIC ALGORITHM II

Multi-objective optimization using evolutionary algorithms (MOEA) is an approach which optimizes multiple objectives concurrently without costing on individual criterion. Many variants of MOEA, which are

Table 2: Results using preference based MOP

	Priorities	Global Condition Number	Workspace Utilization (%)	Stiffness (N/m)	Max. Force Norm (N)	Normalized Moment Error (Nm)	Max. Actuator Force (N)
I	$w_1 = 0.5$; $w_2 \dots w_6 = 0.1$	**2.12**	83.80	293.00	386.98	0.83	610.76
II	$w_2 = 0.5$; $w_1, w_3, \dots w_6 = 0.1$	3.71	**95.00**	125.60	431.20	0.36	648.19
III	$w_3 = 0.5$; $w_1, w_2, w_4 \dots w_6 = 0.1$	2.17	82.00	**357.14**	360.85	0.37	554.39
IV	$w_4 = 0.5$; $w_1, w_2, w_3, w_5, w_6 = 0.1$	3.29	85.35	200.00	**349.21**	0.30	**471.31**
V	$w_5 = 0.5$; $w_1, w_2, w_3, w_4, w_6 = 0.1$	3.10	85.30	191.30	360.93	**0.24**	**484.03**
VI	$w_6 = 0.5$; $w_1, w_2, w_3, w_4, w_5 = 0.1$	3.79	81.62	155.25	402.69	1	514.81
VII	$w_{1-6} = 0.167$	2.59	92.05	231.55	377.59	0.43	526.96

of preferences for dissimilar objectives [44]. Normally, the selection of preferences is either based on trial and error experiments or on the perceptive judgment of the end user. Such preference selection are subjective and do not have a logical base. Moreover dissimilar quality measures of different units and scales are added or multiplied in a single objective function which is not correct mathematically. Results from preference based MOP have been provided in the Table 2. Here case I to VI refer to instances wherein individual objectives are preferred over rest and case VII indicates results when all the objectives are given equal priorities. Results for the best objective values are shown in the bold face; these values have been obtained when the corresponding

based on the Pareto front approach, have been proposed by researchers such as NSGA (non-dominated sorting genetic algorithm), NPGA (Niched Pareto genetic algorithm), SPEA (strength Pareto evolutionary algorithm) and MOMGA (multi-objective messy genetic algorithm) [44]. Despite different strategies used in these algorithms, they essentially work with population of solutions and their inherent mechanism of evolution emulates the natural evolution. The evolution mechanism further facilitates exploration of various trade-off solutions with different grades and blends of objectives. Moreover EA does not require derivatives of objective functions and has robust operators such as reproduction and regeneration to avoid convergence to

local optima. Applications ranging from engineering design, groundwater monitoring, and autonomous vehicle navigation to polymer extrusion and city planning have been benefited significantly by use of EA [44, 45].

The most popular of the MOEA is the non-dominated sorting algorithm (NSGA II) which is the most efficient optimization routine as maintained by researchers [46]. Consequently the NSGA II is implemented and investigated for its significance in the present research. The idea of Non-dominated Pareto hypersurface solutions proposed by [47] is used in most of the MOP's wherein two solutions are compared and the non-dominated one is selected. A non-dominated solution is the one which is not worse than the other solution being compared with, in terms of all the objectives and is strictly better in at least one objective. NSGA II uses three important operators namely, selection, crossover, mutation and crowding distance. The selection or reproduction operator facilitates competent solutions and creates their multiple copies while eliminating less competent solutions from the mating pool of solutions. Crossover operator is responsible for creation of new solutions by combining good substrings from parent populations. To further improve solutions a local search is performed using mutation operator. If the mutation is carried out at the first place of the binary solution, the mutation operator may also help in maintaining diversity in the population by changing solutions values to a large extent. Crowding distance is another operator used to maintain diversity among solutions by supporting distant solutions. For the details scheme of NSGA II [48, 49] are recommended.

Design optimization was carried out using NSGA II algorithm. Essential parameters of NSGA II, used while implementation, were [49], population size: 1000; crossover probability: 0.95; real-parameter mutation probability: 0.05; distribution index for crossover: 10; distribution index for mutation: 50.

After only five iterations, all the fifty solutions evolved and completely filled the first non-dominated front. In other words all these fifty solutions or robot designs, after evolution for five iterations, became non-dominated. To study the behaviour of other objectives with condition number values, nominal values of the objectives functions of all fifty non-dominated solutions have been plotted against their normalized condition number values (Fig. 7). Arrows pointing upward in the figure window of an objective indicate maximization requirement while arrows pointing down indicate minimization aim for that objective function. For a quick glance at the optimized design solutions, the first ten design solutions out of fifty non-dominated solutions have also been listed in Table 3. Here angular and linear positions of the actuator connection points are displayed in radians and meters respectively. All these design solutions are either better or equal to other solutions in terms of all the six objective functions. Although all fifty Pareto optimal designs are non-dominated and thus are equally good, they provide different values for the six objective functions. The maximum actuator force was a major design constraint and as can be seen, this objective has been improved using NSGAII approach. While using single objective optimization, the maximum actuator force requirement was 645.19 N which was reduced after preference based optimization to 471.31 N. However, after NSGAII based multiobjective optimization, design solutions have been obtained which can provide us a further low value of maximum actuator force as 255.4 N. The results obtained in this research exhibit an expected relation among various objectives. It has been shown [39] that the value of maximum actuator forces can be reduced by minimizing the condition number thus when the condition number is minimized, the actuator force requirements also gets reduced to some extent. This statement is evident from the results displayed in Fig.7.

Further, stiffness in the task space is computed from actuator stiffness's using Jacobian matrix of the robot

Table 3: Optimized design parameters for the first ten Pareto designs along with their performance indices

q1	q2	q3	q4	q5	q6	q7	q8	F1	F2	F3	F4	F5	F6
0.864278	0.116993	0.844909	0.154361	1.199843	0.115637	1.176933	0.117437	2.664334	1	312.918	176.2088	1.6E-14	255.4224
0.695503	0.10639	0.687118	0.143618	1.244158	0.106223	1.138916	0.104468	2.659987	0.969697	236.2233	193.9984	2.760619	255.4224
0.970765	0.10764	0.687118	0.143077	0.947606	0.10738	1.159404	0.104453	3.387852	1	121.2046	223.4728	1.311769	257.3365
1.011875	0.105391	0.73375	0.157801	0.955532	0.104644	0.966883	0.1096	5.267333	1	62.99519	213.5579	1.30E-14	274.9148
0.681357	0.116625	0.733738	0.157801	0.955532	0.104644	0.966831	0.1096	2.548427	1	184.3358	172.9176	1.07E-14	274.997
1.011875	0.105392	1.030884	0.15667	1.117269	0.118608	1.178231	0.114286	5.234709	0.909091	88.3244	195.3923	8.88E-15	452.9552
0.8319	0.106015	0.733738	0.15667	1.117269	0.11845	1.182643	0.114286	2.392176	0.909091	360.8966	184.9161	1.60E-14	452.9552
0.690724	0.112105	0.733738	0.156827	1.117269	0.11845	1.182643	0.114286	2.339801	0.939394	362.1459	178.1706	1.21E-14	453.1048
0.665066	0.109561	0.677967	0.15748	0.877682	0.106278	1.188734	0.113638	2.193216	1	293.4999	198.5656	9.47E-15	495.5811
0.689586	0.10539	0.831864	0.157801	0.955532	0.104644	0.966848	0.1096	3.446526	1	113.4533	184.5927	1.56E-14	274.9821

(32). Thus stiffness improves when the Jacobian matrix is well conditioned and vice versa (Fig.7). Similarly Maximum of actuator forces also shows an expected positive correlation with stiffness. It is evident from these illustrations that the solutions are converging towards improved values of the objectives. The selection operator of NSGA II contributes positively by selecting vital few from useful many solutions.
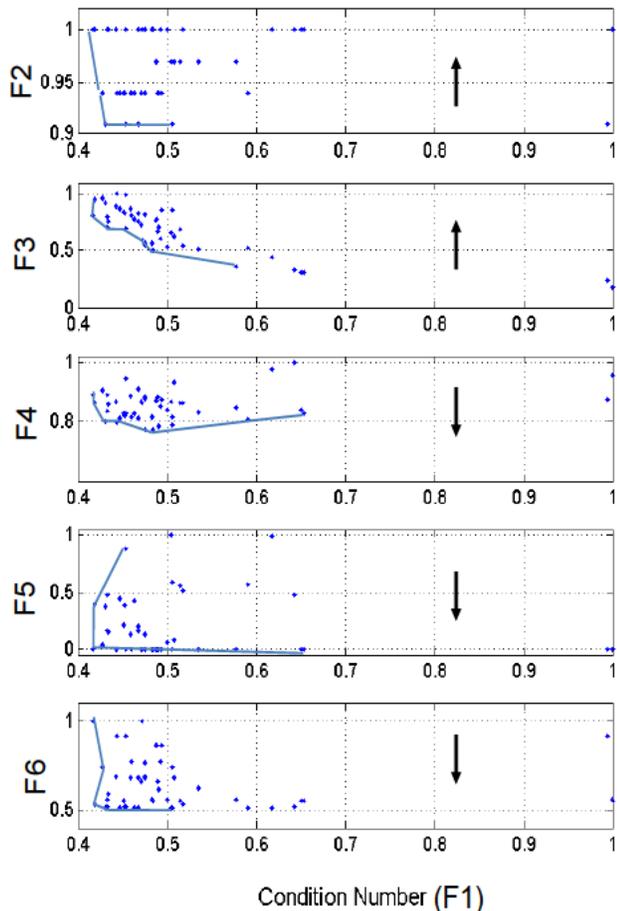
Figure 7: Normalized objectives versus normalized condition number values (F1: condition number, F2: workspace utilization, F3: stiffness N/m, F4: max. force norm, F5: normalized moment error in realizing moment with positive forces & F6: max. actuator force)

Final design solutions (fifty solutions), obtained through NSGA II, are found to abide by all the constraints (1-3) and thus are feasible.

V. FUZZY BASED FINAL RANKING SELECTION METHOD

Subsequent to the application of NSGAII, a set of non dominating solutions is obtained wherein all the solutions are equally competetive and good. However, pragmatically, the designer needs only one solution to any design problem in a given instance and therefore has to make a decision on selection of a final solution. This amounts to a big cognitive load on the designer and apparently certain tools are required at this stage to help the designer in making this crucial decision. Some work

has been done by researchers in the past wherein fuzzy inferencing is preponderantly used to select the best solution from the finally obtained Pareto solutions [43, 50]. In the present work also a fuzzy based approach has been applied in order to select the final solution from the Pareto solutions. The method used has been described below detailing various steps used.

1) Fuzzification:

Initially all the six objctive functions are defined as fuzzy numbers and the universe of discourse or the range of each of the variables is decided by the values obtained from the experiments caried out during optimization using evolutionary algorithm NSGAII. Each of the six fuzzy objective functions are represented by four fuzzy membership functions namely; Low (L), Medium (M), High (H) and Very High (VH) as shown in Figure 8.

2) Fuzzy Inference:

The next step after input (objectives) fuzzification is to compute the fuzzy inference output for given inputs. Inference mechanism of Fuzzy systems is implemented through its rule-base which is a collection of *if and then* rules connecting the *antecedent* (input) and *consequent variables* (output). General structure of a rule-base is given by as shown below.

If f_1 is MF_{i1} and, ... and f_N is MF_{im} then AS_i is y_i

Here f_1... f_N are the objectives as inputs to the fuzzy system, *m* is the index for the Membership function level, MF_{i1} ....MF_{im} are the Membership functions corresponding to objectives, AS_i is the activation score for i^{th} rule and its numerical value is y_i. Total number of rules N_R is derived from the number of MFs along with the antecedent variables and is given by following relation [39].

$$N_R = \prod_{j=1}^{N} M_j \qquad (35)$$

Once again here, *j* is the index for the objective function; *N* stands for the total number of objective functions, and M_j is the total number of Membership functions for objective function *j*. Thus, when six objectives are represented using four Membership functions (as shown in Figure 8), a total of 4^6 i.e. 4096 rules are formed. These rules are the combination of all possible arrangements of Membership functions of the six objectives. Certain example rules are shown below in the Table 4 along with their consolidated rule outputs. While finding the rule outputs their antecedent MFs are given some numerical values as L (Low) = 0; M (Medium) =1; H (High) =2; VH (Very High) =3.

The outputs for these rules are simply the sum of the membership scores of their constituent *MFs*.

Standard procedure to find output from fuzzy system is then followed, wherein weights of objectives for each

rule can be computed by considering the product of all applicable Membership functions degrees of fulfillment.
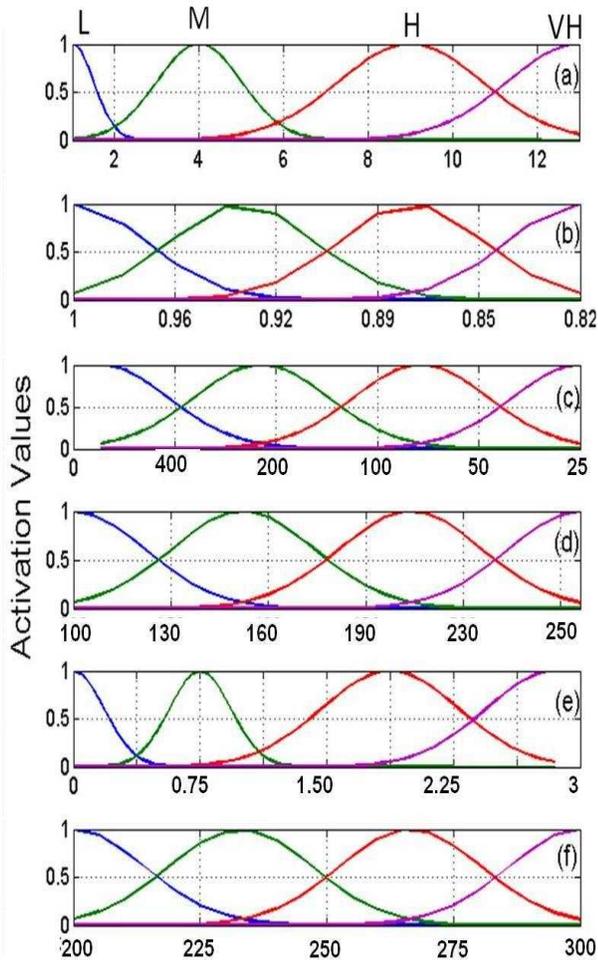
Figure 8: Fuzzy objectives (a) Condition number (b) Robot workspace (c) Stiffness, N/m (d) Norm of actuator forces, N (e) Moment error, Nm (f) Maximum actuator force, N

Table 4: Example rule base for the fuzzy based final ranking selection

Rule no	F1	F2	F3	F4	F5	F6	Rule output
1	L	L	L	L	L	L	00+1=01
2	L	M	M	M	M	M	05+1=06
3	M	H	M	L	H	VH	09+1=10
4	M	L	H	M	L	H	06+1=07
5	H	VH	L	H	M	L	08+1=09
6	H	M	VH	L	H	M	09+1=10
7	H	H	H	VH	L	H	11+1=12
8	VH	M	VH	L	H	M	10+1=11
9	VH	VH	L	H	M	VH	12+1=13
10	VH	VH	VH	VH	VH	VH	18+1=19

Degrees of fulfillment can be computed using (36) and weights are found using by (37). Here f_j is the input objective value and N stands for the number of

objectives. Note that $\bar{f}_{ij}$ and σ_{ij} are the mean and standard deviation of the individual Gaussian membership functions m_{ij} and are plotted as fuzzy functions based on the limiting values $(f_{max} - f_{min})$ of objectives.

$$AF_{ij}(f_j, \bar{f}_{ij}, \sigma_{ij}) = ae^{-\frac{(f_j - \bar{f}_{ij})^2}{2\sigma_{ij}}} \quad (36)$$
$$w_i = \prod_{j=1}^{N} AF_{ij} \quad (37)$$

Numerical or crisp output of the fuzzy inference or the overall membership score of a solution is the weighted average of all the individual rule consequents for this given set of objective values. The overall Membership score (OAS) can be computed using (38) as shown below.

$$Y = \frac{\sum_{i=1}^{Nr}(w_i y_i)}{\sum_{i=1}^{Nr} w_i} \quad (38)$$

The fuzzy index Y^* for a solution can then be obtained from this crisp output using (39), where floor(.) is used to represent the function which returns the integer which is less than or equal to the argument.

$$Y^* = floor(Y) \quad (39)$$

All fifty non dominated solutions obtained through NSGAII implementation are set as inputs to the above described fuzzy selection system and the outputs obtained subsequently are recorded. Five sample design solutions have been shown in Table 5, along with their respective objective function values and fuzzy indices. Design solution number one (Table 5) has been finally selected for the proposed robot design since this solution has minimum fuzzy index value. It may be emphasized here that though all the solutions are non-dominated and should be equally good, their fuzzy indices are different. This may also be concluded that the fuzzy ranking and selection method is able to provide better discrimination among solutions and thus the one with minimum fuzzy index is better than rest of the solutions.

Table 5: Example rule base (five solutions shown) for the fuzzy based final ranking selection using Overall Fuzzy Index (O.F.I.)

F1	F2	F3	F4	F5	F6	O.F.I.	O.F.I. (Integer)
2.66	1	313	176	1.6E-14	255	1.20	1
2.65	0.96	236	194	2.76	255	4.62	4
3.38	1	121	223	1.3E-14	257	4.10	4
5.26	1	63	214	1.1E-14	275	5.15	5
2.5	1	184	173	8.9E-15	275	2.05	2

The solution with lowest fuzzy index has also been illustrated in Figure 9.
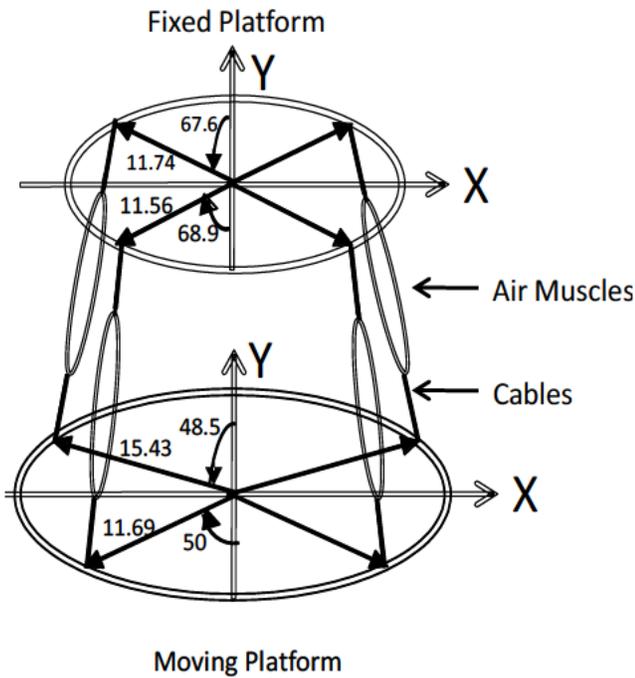
Figure 9: An instance of Non-dominating Ankle robot design acquired using NSGA II

VI. RESULTS AND DISCUSSION

Systematic design analysis of the parallel robot was carried out and performance indices at different stages of the analysis were formulated. Initially the design optimization was performed following the past practice wherein only the condition number of the robot's jacobian matrix is minimized. Genetic algorithm was used as the tool and the optimized values for all the objectives were obtained. These values have been shown in Table 1. It is apparent from the results that while the condition number value is low (2.06), the required value of the norm of the actuator forces is undesirably high (645.19). For the ankle robot which is being designed for the medical purpose, better workspace utilization and smaller values for the actuator forces are essential and hence as a next step, a preference based multi-objective optimization was conducted to obtain a Pareto hyper-surface of the objective functions. The objectives were all combined by varying their weights into a single objective function. Once again GA was used to optimize the single objective which blends all the design objectives. Results obtained from the consequence of the optimization have been displayed in the Table 2. As can be seen from this table, design solutions failed to provide complete utilization of the workspace and also indicate higher values for the maximum actuator force requirement. In one of the set of weights (second row of the Table 2), workspace utilization index was given 50% weight while other objectives were given only 10% and yet the space utilization obtained was only 95% while

the maximum actuator force required to be 648.19 N. These results suggest that the weights for important objectives are required to be increased but that has to be done on the cost of other objectives and therefore this approach cannot be acceptable. Finally, the evolutionary optimization approach was adapted and NSGA II algorithm [47], owing to its much popularity and effectiveness, was coded in Matlab software to solve the present problem of parallel robot design optimization. Binary tournament selection operator was used to pick solutions from the combined population of parents and offspring solutions based on their non-dominating ranks. While carrying out the NSGA-II approach, fifty binary solutions were generated simultaneously and randomly using Knuth's random number generator [51]. Six objective functions evaluated were global condition number, workspace index, Robot's stiffness, norm of the actuator forces, error in the moments realized at the MP to achieve tensionability, and the maximum actuator force. As a result of the optimization through NSGAII, non-dominated set of solutions was obtained and apparently design solutions thus obtained, provided better objective values aiding imposed constraints. Finally, to pick a single design solution from fifty non-dominating solutions, a fuzzy based selection scheme is used. Apparently, the fuzzy selection scheme works quite well and this fact is evident from the analysis of objective values from the selected solution.

VII. CONCLUSIONS

A wearable parallel robot for ankle joint rehabilitation has been conceptualized after carefully studying t the best he existing ankle robot designs. The ankle robot is based on a parallel mechanism and has been designed to be compact and kinematically compliant to the ankle joint motions. Pneumatic muscle actuators are used in this robot, owing to their high power to weight ratio and intrinsic compliant actuation. On account of the challenges imposed by wearability requirement, cable based actuation, use of parallel mechanism, flexible actuators and clinical requirements for ankle joint rehabilitation treatments, the robot design was required to be analyzed and optimized.

Subsequently, design analysis was performed by studying three main design levels of the robot and performance objectives were identified to closely define these design hierarchies. The first design level was the *kinematic design stage* comprising of optimization of condition number of the robot's Jacobian matrix and computation of the workspace as the performance objectives at this design level. *Actuator design* is the second stage wherein the force closure has been solved following the constraints imposed by the cable based actuation. Norm of the actuator forces in the entire

workspace of the robot has also been minimized. Finally in the third design level, the structural analysis is performed wherein performance objectives such as stiffness and rigidity of the robot are analyzed. Ankle robot design was defined in terms of the position vectors of its actuator connection points which were altered to obtain newer robot designs. Initially the optimization was performed using a single objective optimization approach. However in view of the fact that multiple objectives were required to be optimized simultaneously, a preference based approach and evolutionary algorithm based NSGA II algorithm were adapted to solve the present design optimization problem. Comparing results from NSGA II and the results obtained from the single objective optimization and preference based optimization approaches it is apparent that NSGA II is able to provide better design solutions by simultaneously optimizing objectives. Nevertheless, there are certain challenges which NSGA II algorithm faces and the same have been observed in the present research. It is proposed that these research questions may be potentially considered for a future research endeavor.

a) As NSGA II algorithm progresses more and more solutions become non-dominated during selection and this makes the algorithm progressively inefficient especially while dealing with large number of objectives.

b) NSGA II algorithm lacks a clear termination criterion.

c) User preference cannot be included in the algorithm; preferred solutions are selected using a posteriori approach.

Fuzzy based ranking method which was devised and implemented in order to select the final design solution from the set of non-dominated solution set was able to provide better discriminate among the solutions. The finally selected design solution has been found to be providing improved objective values.

REFERENCES

[1]   M. J. Girone, G. C. Burdea, and M. Bouzit, "'Rutgers ankle' orthopedic rehabilitation interface," American Society of Mechanical Engineers, Dynamic Systems and Control Division (Publication) DSC, vol. 67, pp. 305-312, 14 November 1999 through 19 November 1999 1999.

[2]   J. S. Dai, T. Zhao, and C. Nester, "Sprained Ankle Physiotherapy Based Mechanism Synthesis and Stiffness Analysis of a Robotic Rehabilitation Device," Autonomous Robots, vol. 16, pp. 207-218, 2004.

[3]   J. A. Saglia, N. G. Tsagarakis, J. S. Dai, and D. G. Caldwell, "Control strategies for ankle rehabilitation using a high performance ankle exerciser," in Robotics and Automation (ICRA), 2010 IEEE International Conference on, pp. 2221-2227.

[4]   J. Yoon, J. Ryu, and K. B. Lim, "Reconfigurable ankle rehabilitation robot for various exercises," Journal of Robotic Systems, vol. 22, pp. S15-S33, 2006.

[5]   G. Liu, J. Gao, H. Yue, X. Zhang, and G. Lu, "Design and kinematics simulation of parallel robots for ankle rehabilitation," in 2006 IEEE International Conference on Mechatronics and Automation, ICMA 2006, 2006, pp. 1109-1113.

[6]   C. E. Syrseloudis and I. Z. Emiris, "A parallel robot for ankle rehabilitation-evaluation and its design specifications," in 8th IEEE International Conference on BioInformatics and BioEngineering, BIBE 2008, 2008.

[7]   J. L. Pons, "Rehabilitation exoskeletal robotics," IEEE Engineering in Medicine and Biology Magazine, vol. 29, pp. 57-63, 2010.

[8]   M. Ardalani-Farsa and S. Zolfaghari, "Chaotic time series prediction with residual analysis method using hybrid Elman-NARX neural networks," Neurocomputing, vol. 73, pp. 2540-2553.

[9]   S. Khatami and F. Sassani, "Isotropic design optimization of robotic manipulators using a genetic algorithm method," in IEEE International Symposium on Intelligent Control - Proceedings, Vancouver, 2002, pp. 562-567.

[10] L. W. Tsai and S. Joshi, "Kinematics and optimization of a spatial 3-UPU parallel manipulator," Journal of Machine Design, vol. 122, pp. 439-446, 2000.

[11] Y. X. Su, B. Y. Duan, and C. H. Zheng, "Genetic design of kinematically optimal fine tuning Stewart platform for large spherical radio telescope," Mechatronics, vol. 11, pp. 821-835, 2001.

[12] M. Stock and Miller K., "Optimal kinematic design of spatial parallel manipulators," Transactions of ASME, vol. 125, pp. 292-301, 2003.

[13] J. P. Merlet, "Determination of the optimal geometry of modular parallel robots," Proceedings of the 2003 IEEE International Conference on Robotics & Automation, pp. 1197-1202, September 14-19, Taipei, Taiwan. 2003.

[14] X. J. Liu, "Optimal kinematic design of a three translational DoFs parallel manipulator," Robotica, vol. 24, pp. 239-250, 2006.

[15] S. Sergiu, V. Maties, and R. Balan, "Optimization of workspace of a 2 DOF parallel robot," Proceedings of the 2006 IEEE, International Conference on Mechatronics and Automation, pp. 165-170, June 25 - 28, 2006, Luoyang, China. 2006.

[16] M. Hassan and A. Khajepour, "Optimization of actuator forces in cable-based parallel manipulators using convex analysis," IEEE Transactions on Robotics, vol. 24, pp. 736-740, 2008.

[17] F. Hao and J. P. Merlet, "Multi-criteria optimal design of parallel manipulators based on interval analysis," Mechanism and Machine Theory, vol. 40, pp. 157-171, 2005.

[18] J. Lemay and L. Notash, "Configuration engine for architecture planning of modular parallel robots," Mechanism and Machine Theory, vol. 39, pp. 101-117, 2004.

[19] R. Unal, G. Kiziltas, and V. Patoglu, "Multi-criteria design optimization of parallel robots," in 2008 IEEE International Conference on Robotics, Automation and Mechatronics, RAM 2008, 2008, pp. 112-118.

[20] T. Erfani and S. V. Utyuzhnikov, "Directed search domain: a method for even generation of the Pareto frontier in multiobjective optimization," Engineering Optimization, vol. 43, pp. 467-484, 2011/07/10.

[21] E. Courteille, D. Deblaise, and P. Maurine, "Design optimization of a delta-like parallel robot through global stiffness performance evaluation," in 2009 IEEE/RSJ International Conference on Intelligent Robots and Systems, IROS 2009, 2009, pp. 5159-5166.

[22] S. D. Stan, V. Maties, and R. Balan, "Genetic algorithms multiobjective optimization of a 2 DOF micro parallel robot," in Proceedings of the 2007 IEEE International Symposium on Computational Intelligence in Robotics and Automation, CIRA 2007, Jacksonville, FL, 2007, pp. 522-527.

[23] I. Tyapin and G. Hovland, "Multi-objective design optimisation of a class of PKMS - The 3-DOF gantry-TAU," in Proceedings of the IASTED International Conference on Modelling, Identification and Control, 2010, pp. 255-262.

[24] G. Coppola, D. Zhang, and K. Liu, "A 6-DOF reconfigurable hybrid parallel manipulator," Robotics and Computer-Integrated Manufacturing, vol. 30, pp. 99-106, 2014.

[25] G. Cui, H. Zhou, N. Wang, and H. Zhang, "Multi-objective optimization of 3-UPS-S parallel mechanism based on isight," Nongye Jixie Xuebao/Transactions of the Chinese Society for Agricultural Machinery, vol. 44, pp. 261-266, 2013.

[26] Q. M. Meng, "Design of a parallel manipulator based on multi-objective self-adaptive differential evolution algorithm," Applied Mechanics and Materials, vol. 328, pp. 3-8, 2013.

[27] G. Zhen and Z. Dan, "Workspace Representation and Optimization of a Novel Parallel Mechanism with Three-Degrees-of-Freedom," Sustainability vol. 3, pp. 2217-2228, 2011.

[28] B. Dasgupta and T. S. Mruthyunjaya, "Stewart platform manipulator: A review," Mechanism and Machine Theory, vol. 35, pp. 15-40, 2000.

[29] J. Pusey, A. Fattah, S. Agrawal, and E. Messina, "Design and workspace analysis of a 6-6 cable-suspended parallel robot," Mechanism and Machine Theory, vol. 39, pp. 761-778, 2004.

[30] R. Boudreau and N. Turkkan, "Solving the forward kinematics of parallel manipulators with a genetic algorithm," Journal of Robotic Systems, vol. 13, pp. 111-125, 1996.

[31] J. K. Salisbury and J. J. Craig, "Articulated hands-force control and kinematic issues," International Journal of Robotics Research, vol. 1, pp. 4-17, 1982.

[32] R. Kurtz and V. Hayward, "Multiple-goal kinematic optimization of a parallel spherical mechanism with actuator redundancy," IEEE Transactions on Robotics and Automation, vol. 8, pp. 644-651, 1992.

[33] T. Huang, C. M. Gosselin, D. J. Whitehouse, and D. G. Chetwynd, "Analytical approach for optimal design of a type of spherical parallel manipulator using dexterous performance indices," Proceedings of the Institution of Mechanical Engineers, Part C Journal of Mechanical Engineering Science, vol. 217, pp. 447-456, 2003.

[34] S. Behzadipour and A. Khajepour, "Stiffness of cable-based parallel manipulators with application to stability analysis," Journal of Mechanical Design, Transactions of the ASME, vol. 128, pp. 303-310, 2006.

[35] C. M. Gosselin and E. Lavoie, "On the kinematic design of spherical three-degree-of-freedom parallel manipulators," International Journal of Robotics Research, vol. 12, pp. 394-402, 1993.

[36] J. J. Moré and G. Toraldo, "Algorithms for bound constrained quadratic programming problems," Numerische Mathematik, vol. 55, pp. 377-400, 1989.

[37] M. Krefft and J. Hesselbach, "Elastodynamic optimization of parallel kinematics," in Proceedings of the 2005 IEEE Conference on Automation Science and Engineering, IEEE-CASE 2005, Edmonton, 2005, pp. 357-362.

[38] J. Pusey, A. Fattah, S. Agrawal, and E. Messina, "Design and workspace analysis of a 6-6 cable-suspended parallel robot," Mechanism and Machine Theory, vol. 39, pp. 761-778, 2004.

[39] P. K. Jamwal, S. Xie, and K. C. Aw, "Kinematic design optimization of a parallel ankle rehabilitation robot using modified genetic algorithm," Robotics and Autonomous Systems, vol. 57, pp. 1018-1027, 2009.

[40] G. Mroz and L. Notash, "Design and prototype of parallel, wire-actuated robots with a constraining linkage," Journal of Robotic Systems, vol. 21, pp. 677-687, 2004.

[41] Colbrunn R. W., Nelson G. M., and Quinn R. D., "Modeling of Braided Pneumatic Actuators for Robotic Control," Proceedings of the International Conference on Intelligent Robots and Systems, vol. Oct 29th - Nov.03rd ,2001., 2001.

[42] S. Y. Shin, I. H. Lee, Y. M. Cho, K. A. Yang, and B. T. Zhang, "EvoOligo: Oligonucleotide probe design with multiobjective evolutionary algorithms," IEEE Transactions on Systems, Man, and Cybernetics, Part B Cybernetics, vol. 39, pp. 1606-1616, 2009.

[43] C. Kahraman, S. Birgün, and V. Z. Yenen, "Fuzzy multi-attribute scoring methods with applications," Fuzzy Multi-Criteria Decision Making, vol. 16, pp. 187-208, 2008.

[44] Coello C. A. C. and Lamont G. B., "Applications of multi-objective evolutionary algorithms," World Scientific, vol. ISBN 981-256-106-4 Singapore, 2004.

[45] Z. G. Hou, L. Cheng, and M. Tan, "Multicriteria optimization for coordination of redundant robots using a dual neural network," IEEE Transactions on Systems, Man, and Cybernetics, Part B Cybernetics, vol. 40, pp. 1075-1087, 2010.

[46] R. R. Chan and S. D. Sudhoff, "An Evolutionary Computing Approach to Robust Design in the Presence of Uncertainties," IEEE Transactions on Evolutionary Computation, 2010.

[47] K. Deb, Multi-Objective Optimization using Evolutionary Algorithms: John Wiley & sons, Ltd, 2004.

[48] K. Deb, A. Pratap, S. Agarwal, and T. Meyarivan, "A fast and elitist multiobjective genetic algorithm: NSGA-II," IEEE Transactions on Evolutionary Computation, vol. 6, pp. 182-197, 2002.

[49] K. Deb and S. Tiwari, "Multi-objective optimization of a leg mechanism using genetic algorithms," Engineering Optimization, vol. 37, pp. 325-350, 2005.

[50] B. J. Reardon, "Fuzzy logic versus niched Pareto multiobjective genetic algorithm optimization," Modelling and Simulation in Materials Science and Engineering, vol. 6, pp. 717-734, 1998.

[51] D. E. Knuth, The art of computer programming vol. 02, 2000.